# Large Amplitude Out-of-Plane Vibrations of 1,3-Benzodioxole in the $S_0$ and $S_1$ States: An Analysis of Fluorescence and Excitation Spectra by ab Initio Calculations

**Emanuela Emanuele and Giorgio Orlandi***

*Department of Chemistry "G. Ciamician", University of Bologna, 40126 Bologna, Italy*

*Received: March 2, 2005; In Final Form: May 24, 2005*

We report the analytical expressions of the two-dimensional potential energy surfaces (PES) spanned by the puckering and flapping vibrations in the $S_0$ and $S_1$ states of 1,3-benzodioxole (BDO). Both PES are obtained from $S_0$ and $S_1$ energies computed on a grid of 2500 molecular geometries at the CASPT2 level. Both the $S_0$ and $S_1$ PES are anharmonic, and the planar geometry corresponds to a barrier that separates two minima at nonplanar geometries along the puckering/flapping deformations. Eigenvalues and eigenvectors of the mixed puckering/flapping modes are calculated by the Meyer flexible model. Improved vibronic levels, in better agreement with the observed spectra, are obtained by suitably optimized CASPT2 surfaces. To assign the lower-energy (0−500 $cm^{-1}$) portion of emission and absorption spectra, we evaluate the band intensities by estimating the Franck−Condon factors between the puckering/flapping eigenvectors of the $S_0$ and $S_1$ states. From these calculations, we obtain a satisfactory assignment of the ground state IR spectra and of the fluorescence excitation spectrum. Both assignments are supported by the analysis of the vibrational structures of several single vibronic level (SVL) fluorescence spectra. The successful interpretation of these spectra shows that the $S_0$ and $S_1$ PES that we derive for BDO are substantially correct. The barrier heights in the two states are similar: 125.7 and 190.4 $cm^{-1}$ in $S_0$ and in $S_1$, respectively. In $S_0$, the barrier is associated essentially with the puckering motion. In $S_1$, it involves to a considerable extent also the flapping coordinate, whose vibrational frequency is much lower in $S_1$ than in $S_0$. This fact introduces a substantial Duschinsky effect in the $S_0-S_1$ transitions of BDO.

## 1. Introduction

The 1,3-benzodioxole (BDO) molecule has attracted considerable attention[1−10] because it can serve as a model system for conformational studies of larger molecules. The BDO molecule, which is shown in Figure 1, has an out-of-plane ring puckering vibration of the $CH_2$ group that is highly anharmonic and involves a large amplitude motion on a double-minimum potential, with a barrier to planarity of about 100 $cm^{-1}$. The transitions between the puckering vibrational levels dominate the low-energy portion of IR or Raman spectra. Furthermore, in BDO, there is a second low-frequency mode, of the same $b_1$ symmetry as the puckering mode, namely, the out-of-plane ring flapping (or butterfly motion) of the five-atom ring with respect to the benzene ring. The two modes, which are displayed in Figure 2 together with the $a_2$ ring twisting, are coupled, and the vibrational levels arising from their combination add complexity to the IR and Raman vibrational spectra and to the vibronic structure of electronic spectra.

Molecules such as BDO, which may have more than one stable conformation, may serve as simple models of more complicated systems having a distribution of conformations. Conformational studies are of particular relevance for large molecules that may have different local minima of similar energy on their potential energy surfaces (PES). Each minimum is associated with a different conformer that may show different chemical properties. Examples are proteins, which may exist in many different conformations, and their efficiency in performing their functions is strongly dependent on their structure. In this perspective, molecules such as BDO are[1] simple molecular models of complicated systems having large amplitude motions and a distribution of conformations.

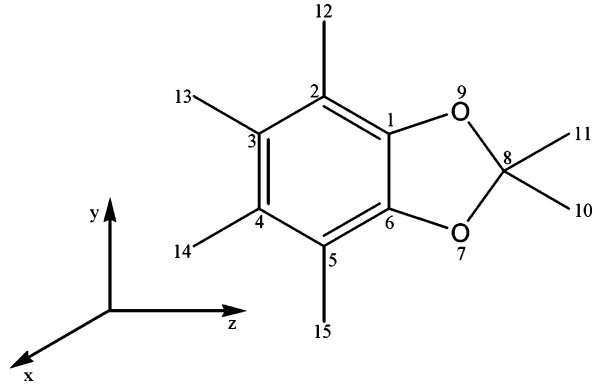


**Figure 1.** Geometry of the BDO molecule with the numbering of the atoms.

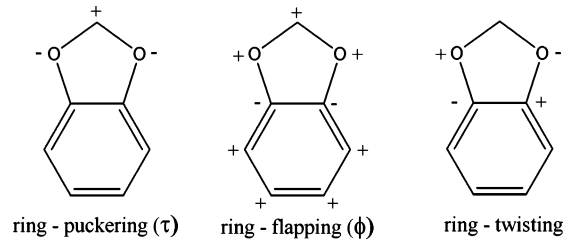


**Figure 2.** Definition of the ring puckering, ring flapping, and twisting coordinates.

Determining the details of the PES of puckering and flapping motions of BDO is equivalent to determining the vibrational

10.1021/jp051055w CCC: $30.25 
Published on Web 06/28/2005

levels of these vibrations and vice versa. Therefore, the measurements of IR and Raman spectra and of vibronic structures of absorption and emission spectra, *together with their proper assignments*, are essential to get valuable information on the PES of BDO large amplitude motions. For these reasons, BDO has been intensely studied by means of spectroscopic and theoretical methods.[1−10]

Duckett et al.[2] measured the gas-phase far IR spectrum of BDO, in the region between 50 and 500 $cm^{-1}$, and interpreted their results by attributing an anharmonic (quadratic plus quartic) potential with the minimum at the planar geometry to the puckering mode.

Alves et al.[3] performed the first investigation of the absorption spectrum of BDO vapor in a cell. The results of their study provided no definitive conclusion about the planarity of this molecule. Later, Hassan and Hollas[4] investigated the $S_1 \leftarrow S_0$ excitation spectrum of BDO using supersonic jet fluorescence spectroscopy and correctly assigned the $S_1 \leftarrow S_0$ origin by identifying it with the 34 780 $cm^{-1}$ band. They also recorded the single vibronic level (SVL) fluorescence spectra emitted from three bands of the excitation spectrum, namely, the origin and the bands at 99 and 204 $cm^{-1}$. They came to the conclusion that the molecule is nonplanar in both the $S_0$ and $S_1$ electronic states and attributed the nonplanarity to a distortion along the lowest-frequency $a_2$ mode, namely, the twisting of the two oxygen atoms that is shown in Figure 1.

Caminati et al.[5] measured the rotational spectra of six vibrational fundamentals and overtones of the isolated molecule in the electronic ground state. By analyzing far IR spectrum of ref 2 by means of Meyer's two-dimensional flexible model[11] and using the highly detailed information obtained from rotational spectroscopy, these authors concluded that the BDO equilibrium structure in $S_0$ is nonplanar, with a barrier of 126 $cm^{-1}$, and that the molecule is subject to deformations along two coordinates, namely, the puckering and flapping motions.

Laane and co-workers[6] investigated the vibrational levels of $S_0$ by measuring the far IR and Raman spectra and by recording SLV dispersed fluorescence spectra emitted from several vibronic levels of $S_1$.[7] Their assignment is fairly similar to that proposed by Caminati et al.[5] but differs in the assignment of the frequency of the flapping mode. They confirmed the notion that the puckering and butterfly modes of BDO strongly interact and obtained a potential energy surface with minima at puckered conformations and with a 164 $cm^{-1}$ barrier at the planar geometry. Furthermore, to explain the bent equilibrium structure of the molecule, they introduced the concept of the anomeric effect, which is based on the electron donation from a lone pair on one oxygen atom to the adjacent carbon−oxygen bond. Since the ring puckering increases the magnitude of the anomeric effect, a nonplanar structure can be stabilized.

The analysis of the $S_0$ vibrational states in the range 0−400 $cm^{-1}$ presented in ref 6 appears to be fairly satisfactory. However, the valuable source of information on ground state vibrational levels that is provided by the high-resolution vibrational structure of SVL fluorescence spectra[6,7] remains to be analyzed and fully exploited.

The knowledge of the vibrational levels of $S_1$ is far less solid than that of $S_0$. The most accurate work so far available is the high-resolution excitation spectrum in a supersonic jet in the region 0−550 $cm^{-1}$ and a room-temperature absorption spectrum in the same spectral interval by Laane and co-workers.[1,8,9,13] These authors proposed assignments for many of the observed vibronic bands, although the information about the vibrational frequencies in $S_1$ is scarce. In fact, because of the absence of IR and Raman spectra in $S_1$, the vibrational frequencies of this state are known only from theoretical calculations, which may not be sufficiently accurate for a reliable assignment of the $S_1$ vibronic structure. Laane and coauthors[9] on the basis of their vibronic assignments concluded that the BDO molecule is nonplanar also in the $S_1$ state, because of deformations along the puckering and flapping coordinates, with a barrier to planarity of 264 $cm^{-1}$ in the $S_1$ state. However, for the reason stated above, we feel that the assignment of the vibronic structure of the $S_1$ state is still an open problem and that the estimate of the $S_1$ barrier ought to be reconsidered.

Very recently, Pietraperzia and coauthors[10] carried out a detailed analysis of some vibronic bands of the $S_1 \leftarrow S_0$ electronic transition by resolving the rotational fine structure. The results of these measurements have evidenced some problems with the assignment of the $S_1 \leftarrow S_0$ vibronic spectrum that were proposed in ref 9. These problems concern specifically the identification of the puckering and flapping fundamentals in the excitation spectrum.

A few theoretical studies[6,9,14] have been devoted to elucidate the conformations and the PES of BDO. The barrier to planarity was found to be 171 $cm^{-1}$ [14] in $S_0$ by MP2/6-31G* calculations. In $S_1$, values of 369 and 516 $cm^{-1}$ [9] were obtained by CIS/6-311+G* and TD-DFT-B3LYP/6-31+G(d) calculations, respectively.

From the summary of previous work, it appears to us that the vibrational structure in the electronic ground state is qualitatively understood, although not yet firmly established. On the contrary, the vibronic structure of anharmonic large amplitude motions in the $S_1$ state does not appear to be assigned in a satisfactory way. This implies that our knowledge of the conformations of BDO in $S_1$ is rather poor.

For this reason, we have performed accurate CASPT2 calculations of the $S_0$ and $S_1$ study with the purpose to provide a reliable picture of the PES along the puckering and flapping coordinates. Then, we have computed the vibrational eigenvalues and eigenvectors in both the $S_0$ and $S_1$ states and the matrix of the $S_0-S_1$ Franck−Condon (FC) factors, which are obviously quite important for the interpretation of the vibronic structure of emission and absorption (or excitation) spectra.

From these calculations, a coherent assignment of the vibrational structures of the excitation spectrum and of several SVL fluorescence spectra has emerged. Therefore, we believe that the presently computed $S_0$ and $S_1$ PES, which appear to be consistent with the available spectroscopic information, are fairly reliable.

## 2. Computational Details

The PES along the puckering and flapping coordinates were calculated using the complete active space self-consistent field (CASSCF) procedure[15] followed by the second-order perturbation theory (CASPT2) employing the MOLCAS-5.2 quantum chemistry program[16] and using contracted basis sets of atomic natural orbitals (ANO).

We calculated the CASPT2 energies of $S_0$ and $S_1$ on a two-dimensional grid of geometries, along the puckering ($\tau$) and flapping ($\phi$) coordinates, for the intervals $-50° < \tau < 50°$ and $-50° < \phi < 50°$, with steps of 2°. The puckering and flapping angles were constrained at the selected values, and every other structural parameter was then optimized at the CASSCF level, for each couple of $\tau$ and $\phi$ values. Subsequently, CASPT2 calculations were performed at the optimized geometry to estimate the effects of dynamic electron correlation.

The crucial step of the calculation is the selection of a proper active space. In general, the active space should include all orbitals with an occupation number different than 2 for occupied orbitals and zero for virtual orbitals. For aromatic systems, the CAS space typically includes the valence $\pi$-orbitals. In this study on the $S_0$ and $S_1$ states of BDO, the active space comprises 14 electrons distributed in 12 orbitals. In all of the geometries considered, the molecule belongs to the $C_s$ point group and the symmetry plane coincides with the *zx* plane. In the planar configuration, the molecule belongs to the $C_{2v}$ point group, whereby the *z* axis is the $C_2$ axis. In the $C_s$ point group, the CAS space includes 7 A′ and 5 A″ orbitals.

The CASPT2 energies calculated on the grid of 2500 geometries were fitted to analytical expressions of the $S_0$ and $S_1$ two-dimensional PES that comprised terms up to the quartic powers of the puckering and flapping coordinates.

The vibrational energies and the eigenvectors for these $S_0$ and $S_1$ PES were obtained by use of Meyer's two-dimensional flexible model.[11]

The FC factors for these two modes were obtained by numerical calculation of the overlaps between the $S_0$ eigenvectors and the $S_1$ eigenvectors.

Calculations of the oscillator strength of $S_0-S_1$ transitions have been made at the CIS/6-31G* level.

## 3. Results

**A. Large Amplitude Modes: The Puckering and Flapping Modes.** Laane and co-workers[6−9] studied intensively the vibrational energy levels of the puckering ($\tau$) and flapping ($\phi$) motions of BDO in both states $S_0$ and $S_1$. In particular, they measured IR, absorption, and fluorescence excitation spectra and single vibronic level fluorescence.

The $S_0$ and $S_1$ states in the point group $C_{2v}$ belong both to the $A_1$ representation, and thus, the $S_1 \leftarrow S_0$ electronic transition is polarized along the *z* axis. The oscillator strength of this transition is 0.074 according to a CIS/6-31G* level calculation. Thus, the $S_0 \rightarrow S_1$ transition is of appreciable intensity, and its vibrational structure will be dominated by the FC factors. The puckering and flapping modes belong to the $b_1$ symmetry species, which comprises the modes ranging from 33 to 39. The puckering and flapping modes are denoted as 39 and 38, respectively. Note that, in previous work,[6−9] for a different choice of Cartesian axes, these modes are assigned to the $b_2$ representation of the group $C_{2v}$.

We have calculated the two-dimensional PES of $S_0$ and $S_1$ at the CASPT2 level, on a grid of 2500 geometries spanning the intervals $-50° < \tau < 50°$ and $-50° < \phi < 50°$. The two $S_0$ and $S_1$ PES are represented by the following analytical expression, comprising quadratic and quartic terms:

$$E(\tau, \phi) = a\tau^2 + b\tau^4 + c\phi^2 + d\phi^4 + e\tau\phi + f\tau^2\phi^2 + g\tau\phi^3$$

Expressing the energy by wavenumbers, the parameters representing the $S_0$ PES have the following values: $a = -0.4517$ cm$^{-1}$ deg$^{-2}$, $b = 4.474 \times 10^{-4}$ cm$^{-1}$ deg$^{-4}$, $c = 3.8623$ cm$^{-1}$ deg$^{-2}$, $d = 4.299 \times 10^{-4}$ cm$^{-1}$ deg$^{-4}$, $e = 0.7075$ cm$^{-1}$ deg$^{-2}$, $f = -1.764 \times 10^{-4}$ cm$^{-1}$ deg$^{-4}$, and $g = -0.182 \times 10^{-4}$ cm$^{-1}$ deg$^{-4}$. For $S_1$, the corresponding parameters are the following: $a = -0.1909$ cm$^{-1}$ deg$^{-2}$, $b = 4.298 \times 10^{-4}$ cm$^{-1}$ deg$^{-4}$, $c = 0.9770$ cm$^{-1}$ deg$^{-2}$, $d = 3.459 \times 10^{-4}$ cm$^{-1}$ deg$^{-4}$, $e = 0.9902$ cm$^{-1}$ deg$^{-2}$, $f = -2.074 \times 10^{-4}$ cm$^{-1}$ deg$^{-4}$, and $g = -2.140 \times 10^{-4}$ cm$^{-1}$ deg$^{-4}$.

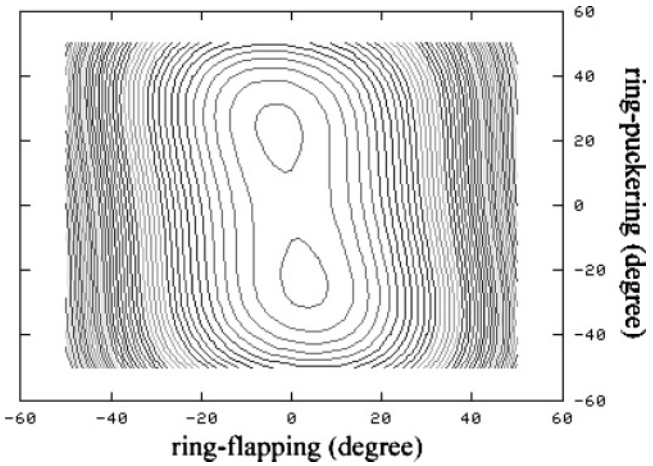


**Figure 3.** CASPT2 PES for the puckering and flapping coordinates in the state $S_0$.

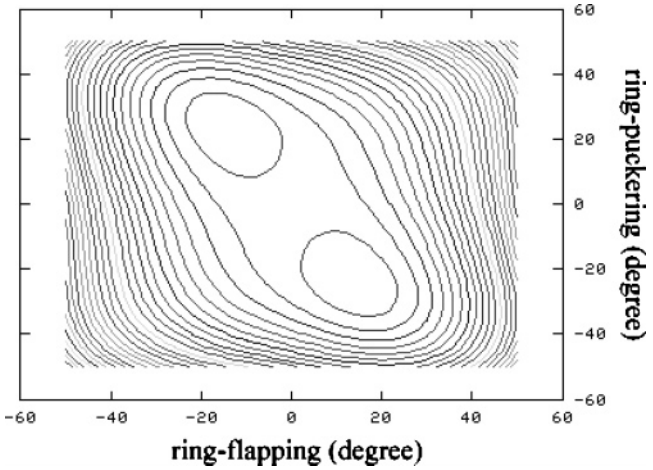


**Figure 4.** CASPT2 PES for the puckering and flapping coordinates in the state $S_1$.

The $E(\tau, \phi)$ potentials for $S_0$ and $S_1$ are shown in Figures 3 and 4. The CASPT2 energy gap between the $S_1$ and $S_0$ minima is 4.33 eV, which is very close to the experimental value 4.31 eV.[4,6]

It is worth noting that the coupling term $\tau\cdot\phi$ is important because it affects significantly the mixing between the two vibration modes and may produce a double-minimum shape even if each individual mode has a single minimum. The presence of coordinates' powers higher than 2 implies that the PES of the puckering and flapping vibrations are anharmonic and that the analysis of vibrational levels cannot be rigorously made in terms of the number of quanta of the one or of the other mode.

The CASPT2 $S_0$ potential shows a double-minimum structure, associated mainly with the puckering mode. The two minima located at $(\tau; \phi) = (+/-22.47°; -/+1.4°)$ from the planar structure and are separated by a barrier of 114.1 cm$^{-1}$ at the planar structure. By comparison, the barrier height that was found by MP2/6-31G* calculations[14] is 171 cm$^{-1}$ and the two minima are located at $(\tau; \phi) = (-/+25°; +/-12°)$.

In the $S_1$ state, the CASPT2 barrier along the puckering coordinate is lower than that in $S_0$; namely, it is 21.2 cm$^{-1}$, and the two minima are located at $-/+14.9°$. However, the barrier on the CASPT2 puckering/flapping PES is 111 cm$^{-1}$ and the two minima are found at $(\tau; \phi) = (+/-22.8°; -/+10.6°)$ along the puckering and flapping coordinates. Thus, the $S_1$ double-minimum structure is due to both coordinates and is

**TABLE 1: Equilibrium Geometry of BDO at the $S_0$ Planar Geometry ($C_{2v}$ Symmetry)[a]**

| state | B3LYP $S_0$ $C_{2v}$ | CASSCF $S_0$ $C_{2v}$ | CASSCF $S_1$ $C_{2v}$ | CIS $S_1$ $C_{2v}$ |
|---|---|---|---|---|
| $C_1-C_2$ | 1.381 | 1.375 | 1.354 | 1.411 |
| $C_2-C_3$ | 1.408 | 1.411 | 1.433 | 1.410 |
| $C_3-C_4$ | 1.394 | 1.391 | 1.444 | 1.419 |
| $C_1-C_6$ | 1.393 | 1.388 | 1.404 | 1.392 |
| $C_1-O_9$ | 1.375 | 1.358 | 1.354 | 1.344 |
| $O_9-C_8$ | 1.432 | 1.407 | 1.405 | 1.405 |
| $C_1C_2C_3$ | 116.73 | 116.54 | 113.96 | 112.86 |
| $C_2C_1C_6$ | 121.99 | 122.22 | 123.64 | 123.89 |
| $C_2C_3C_4$ | 121.28 | 121.25 | 122.40 | 123.25 |
| $C_6C_1O_9$ | 109.75 | 109.02 | 108.73 | 108.95 |
| $C_1O_9C_8$ | 106.07 | 107.09 | 107.25 | 107.38 |
| $O_9C_8O_7$ | 108.35 | 107.79 | 108.04 | 107.33 |
| $H_{10}C_8H_{11}$ | 110.99 | 109.46 | 109.53 | 110.69 |

[a] Bond lengths in angstroms and angles in degrees.

caused to a large extent by the $\tau\cdot\phi$ term in the expression of the potential. Surprisingly, this term is absent in the expression of the $S_1$ potential used in ref 9.

The barrier heights found by Laane et al.[9] by using TD-DFT-BLYP and CIS 6-31G* are 516 and 437 $cm^{-1}$, respectively. We believe that our result obtained at the CASPT2 level is more accurate than the previous theoretical results.

The puckering and flapping vibrational levels found for the CASPT2 $S_0$ and $S_1$ potentials, using Mayer's flexible model, are shown in Tables 2 and 3.

The agreement of the calculated energies with the energies of the observed vibrational levels is good for $S_0$, although the frequency of the flap mode, 245.9 $cm^{-1}$, is lower than the frequency observed in the IR and fluorescence spectra (vide infra). With slight changes in the CASPT2 parameters, we have improved the energies of the vibrational levels. The optimized parameters are the following: $a = -0.473$ $cm^{-1}$ $deg^{-2}$, $b = 4.45 \times 10^{-4}$ $cm^{-1}$ $deg^{-4}$, $c = 4.797$ $cm^{-1}$ $deg^{-2}$, $d = 4.299 \times 10^{-4}$ $cm^{-1}$ $deg^{-4}$, $e = 0.707$ $cm^{-1}$ $deg^{-2}$, $f = -1.764 \times 10^{-4}$ $cm^{-1}$ $deg^{-2}$, $g = -0.182 \times 10^{-4}$ $cm^{-1}$ $deg^{-2}$.

The $S_0$ barrier height obtained with this optimized potential is 125.7 $cm^{-1}$ (increased from the 114.1 $cm^{-1}$ value of the unmodified CASPT2 potential), and the two minima are found at $(\tau; \phi) = (+/-23°; -/+1.4°)$, almost at the same geometries as the minima of the unmodified CASPT2 potential. For comparison, Laane and co-workers[6] deduced from their spectral analysis that the $S_0$ barrier height is 164 $cm^{-1}$ and the two minima are at $(\tau; \phi) = (+/-24°; -/+3°)$. Interestingly, the barrier estimate reported in ref 5 is 126 $cm^{-1}$, that is, very similar to ours.

The vibrational levels found with these potentials, using Mayer's flexible model, are shown in Table 2. The frequency of the flapping mode is now 274.2 $cm^{-1}$, which is close to the frequency inferred from the fluorescence and IR spectra. Also, the frequencies of other levels result in a better agreement with the observed frequencies, as is shown in Table 2. It is worth noting that the eigenvectors of the lower vibrational levels are of definite puckering or flapping character, despite the coupling terms of the potential. In particular, the eigenvector of the 8.7 $cm^{-1}$ level is predominantly based on the puckering, while the eigenvector of the 274.2 $cm^{-1}$ level corresponds exactly to the flapping coordinate. In other words, the two "normal modes" obtained are well described as puckering and flapping, respectively.

In Table 2, we show by comparison the $S_0$ vibrational levels given in ref 6. The levels below 500 $cm^{-1}$ are in substantial agreement with our results. In Table 2, we include also the frequencies $\nu_{14}(a_1)$, $\nu_{37}(b_1)$, and $\nu_{20}(a_2)$, which will be useful in the interpretation of excitation and of SVL spectra.

The vibrational energies calculated by the $S_1$ CASPT2 potential agree qualitatively with the energies observed in the excitation spectrum, although their differences are larger than in the case of $S_0$ (see Table 3). The computed lower fundamental is 21.5 $cm^{-1}$, a value which does not correspond to a band in the excitation spectrum. The computed higher fundamental is 110.5 $cm^{-1}$, and the wavenumber of the $39_2$ level is 119.5 $cm^{-1}$. These two frequencies are to be associated with the energy levels inferred from the hot band observed at 93 $cm^{-1}$ and the cold band observed at 104 $cm^{-1}$, respectively. Assigning the hot band as $39_1{}^0 38_0{}^1$, the inferred energy for the flapping fundamental is $93 + 8.66 \approx 102$ $cm^{-1}$.

**TABLE 2: Calculated and Observed Vibrational Levels of Puckering and Flapping Vibrations in $S_0$**

| numbering of $\nu_{38}/\nu_{39}$ levels, $n$[a] | observed bands[b] ($cm^{-1}$) | inferred frequencies[c] ($cm^{-1}$) | levels of CASPT2[d] PES | levels of optimized[e] PES | assignment of $\nu_{38}/\nu_{39}$ levels | assignment of $\nu_{38}/\nu_{39}$ levels (ref 6) |
|---|---|---|---|---|---|---|
| 1 | | 8.66[f] | 10.7 u | 8.7 | $39^0_1$ | 9.0 |
| 2 | 99 G | 99 | 98.8 g | 98.5 | $39^0_2$ | 100 |
| 3 | 148 H | 157 | 159.2 u | 156.8 | $39^0_3$ | 154 |
| 4 | 236 G | 236 | 230.4 g | 236.0 | $39^0_4$ | 238 |
| 5 | 269 H | 278 | 245.9 u | 274.2 | $38^0_1$ | 267 |
| 6 | 299 G | 299 | 279.4 g | 296.2 | $38^0_139^0_1$ | 299 |
| 7 | 317 H | 325 | 313.8 u | 324.5 | $39^0_5$ | 317 |
| 8 | 380 H | 388 | 374.7 u | 386.6 | $38^0_139^0_2$ | 380 |
| 9 | 403 G | 403 | 386.5 g | 403.9 | $39^0_6$ | 416 |
| 10 | 472 G | 472 | 466.2 g | 472.2 | $38^0_139^0_3$ | 477 |
| 11 | 481 H | 490 | 462.8 u | 489.7 | $38^0_139^0_4$ | 563 |
| 12 | 552 G | 552 | 491.5 g | 545.8 | $38^0_2$ | |
| 13 | | | 522.1 u | 557.5 | $38^0_239^0_1$ | |
| 14 | 583 G | 583 | 550.5 g | 581.7 | $38^0_139^0_5$ | |
| | | 214[b] | | | $20^0_1$ | 214 |
| | | 411[g] | | | $37^0_1$ | 405 |
| | | 534[h] | | | $14^0_1$ | 536 |

[a] The fundamentals of the $\nu_{14}$, $\nu_{37}$, and $\nu_{20}$ vibrations are included, since they are used in subsequent discussions. [b] From refs 6 and 7; G and H indicate cold and hot bands, respectively. [c] From observed bands, by adding the energy of level 1 to the hot band frequencies. [d] Described by the parameters $a = -0.4517$ $cm^{-1}$ $deg^{-2}$, $b = 4.474 \times 10^{-4}$ $cm^{-1}$ $deg^{-4}$, $c = 3.8623$ $cm^{-1}$ $deg^{-2}$, $e = 0.7075$ $cm^{-1}$ $deg^{-2}$; see text. g and u indicate the gerade/ungerade character of eigenvectors. [e] Described by the parameters $a = -0.473$ $cm^{-1}$ $deg^{-2}$, $b = 4.45 \times 10^{-4}$ $cm^{-1}$ $deg^{-4}$, $c = 4.797$ $cm^{-1}$ $deg^{-2}$, $e = 0.707$ $cm^{-1}$ $deg^{-2}$; see text. [f] From ref 12. [g] $\nu_{37} = 409$ $cm^{-1}$ in IR, 419 $cm^{-1}$ in Raman spectra,[7] and 408 $cm^{-1}$ from CASSCF calculations (to be published); we adopt the value 411 $cm^{-1}$. [h] $\nu_{14} = 534$ $cm^{-1}$ in IR.[7]

**TABLE 3: Calculated and Observed Vibrational Levels of Puckering and Flapping Vibrations in $S_1$**

| numbering of $\nu_{38}/\nu_{39}$ levels, $n$[a] | excitation spectrum bands[b] ($cm^{-1}$) | inferred frequencies[c] ($cm^{-1}$) | levels of CASPT2[d] PES | levels of optimized[e] PES | assignment of $\nu_{38}/\nu_{39}$ levels | $\nu_{38}/\nu_{39}$ levels of ref 9 |
|---|---|---|---|---|---|---|
| 1 | 1[f] H | 10 | 21.5 u | 9.0 | $39^1_0$ | 10.9 |
| 3 | 93 H | 102 | 110.4 u | 103.0 | $38^1_0$ | 189.5 |
| 4 | 102 G | 102 | 119.6 g | 98.7 | $39^2_0$ | 101.8 |
| 5 | | | 138.6 g | 150.0 | $39^1_0 38^1_0$ | 204 |
| 7 | 180 H | 188 | 214.1 u | 185.1 | $39^3_0$ | 162.5 |
| 8 | 189 H | 197 | 235.2 u | 213.2 | $39^2_0 38^1_0$ | 297.5 |
| 9 | 204 G | 204 | 220.6 g | 204.4 | $38^2_0$ | 383.1 |
| 10 | 257 H | 266 | 252.7 u | 270.8 | $39^1_0 38^2_0$ | 402.6 |
| 11 | 271 G | 271 | 321.4 g | 272.6 | $39^4_0$ | 273.5 |
| 12 | 290 G | 290 | 340.1 g | 297.6 | $39^2_0 38^2_0$; $39^3_0 38^1_0$ | 400.1 |
| 13 | 301 H | 310 | 331.1 u | 305.3 | $38^3_0$ | |
| 14 | 354 G | 354 | 353.2 g | 346.8 | $39^2_0 38^2_0$ | 504 |
| 15 | 372 H | 381 | 443.8 u | 364.7 | $39^5_0$ | 383.4 |
| 16 | 400 G | 400 | 365.0 g | 408.9 | $38^4_0$; $39^1_0 38^3_0$ | |
| | | 200[b] | | | $20^0_1$ | 200 |
| | | 269[g] | | | $37^0_1$ | 345 |
| | | 464[h] | | | $14^0_1$ | 472[i] |

[a] The fundamentals of the $\nu_{14}$, $\nu_{37}$, and $\nu_{20}$ vibrations are included, since they are used in subsequent discussions. [b] From ref 9; G and H indicate cold and hot bands, respectively. [c] From observed bands, by adding an energy of 8.66 $cm^{-1}$ to the frequencies of hot bands originating from the level $39^0_1$ of the ground state. [d] Described by the parameters $a = -0.1909$ $cm^{-1}$ $deg^{-2}$, $b = 4.298 \times 10^{-4}$ $cm^{-1}$ $deg^{-4}$, $c = 0.977$ $cm^{-1}$ $deg^{-2}$, $e = 0.9902$ $cm^{-1}$ $deg^{-2}$; see text. g and u indicate the gerade/ungerade character of eigenvectors. [e] Described by the parameters $a = -0.2975$ $cm^{-1}$ $deg^{-2}$, $b = 5.82 \times 10^{-4}$ $cm^{-1}$ $deg^{-4}$, $c = 0.505\,25$ $cm^{-1}$ $deg^{-2}$, $e = 0.931$ $cm^{-1}$ $deg^{-2}$; see text. [f] We assume that the band $39^1_1$ lies within the 0−0 band; see text. [g] $\nu_{37} = 315$ $cm^{-1}$ from CIS 6-31G* calculations (to be published); we adopt the value 269 $cm^{-1}$. [h] $\nu_{14} = 514$ $cm^{-1}$ from CIS 6-31G* calculations (to be published); we adopt the value 464 $cm^{-1}$. [i] From CIS 6-31+G* calculations of ref 9.

By slight changes in the CASPT2 potential parameters, we could improve the agreement with the energies of the observed vibrational levels. The parameters have been optimized for the following purposes:

(a) to lower the puckering fundamental from 21.5 $cm^{-1}$ to a value close to 10 $cm^{-1}$, that is, close to the frequency value in the $S_0$ state such that the $39_1^1$ hot band falls within the 0−0 band of the excitation spectrum,

(b) to lower the flapping fundamental from 110.5 $cm^{-1}$ to a value close to 102 $cm^{-1}$, and

(c) to decrease the FC intensity of the 138.6 $cm^{-1}$ g-type band, since in this region of the excitation spectrum no cold band was observed by Laane et al.[9]

The optimized parameters obtained by the optimization procedure are the following: $a = -0.2975$ $cm^{-1}$ $deg^{-2}$, $b = 5.82 \times 10^{-4}$ $cm^{-1}$ $deg^{-4}$, $c = 0.505\,25$ $cm^{-1}$ $deg^{-2}$, $d = 3.5 \times 10^{-4}$ $cm^{-1}$ $deg^{-4}$, $e = 0.931$ $cm^{-1}$ $deg^{-2}$, $f = -2.1 \times 10^{-4}$ $cm^{-1}$ $deg^{-4}$, and $g = -2.1 \times 10^{-4}$ $cm^{-1}$ $deg^{-2}$.

The barrier height obtained with the optimized parameters is 190.4 $cm^{-1}$ (higher than the 111 $cm^{-1}$ barrier obtained from the unmodified CASPT2 potential), and the two minima are found at $(\tau; \phi) = (+/-25.3°; -/+16.0°)$. For comparison, in ref 9, it is estimated that the $S_1$ barrier is 264 $cm^{-1}$ and the two minima are at $(\tau; \phi) = (+/-24°; -/+0°)$.

The vibrational levels found with these potentials, using Mayer's flexible model, are shown in Table 3. The frequency of the lower fundamental is 9.0 $cm^{-1}$, a value that is rather close to the corresponding value in $S_0$. The frequency of the second fundamental is 103.0 $cm^{-1}$, which matches well the frequency inferred from the excitation spectrum. Also, the frequencies of higher levels result in a better agreement with the observed frequencies.

The differences between the $S_0$ and $S_1$ PES, in particular the different positions of the minima, render the eigenvectors of the fundamentals in $S_1$ significantly different from those in $S_0$. This effect is usually referred to as the Duschinsky effect.[17] By inspection of the eigenvectors of the fundamentals, it appears that the $S_1$ normal modes are linear combinations of $S_0$ normal modes, that is, of the puckering and flapping coordinates. The coordinate of the 9.0 $cm^{-1}$ fundamental follows the direction of the two PES minima, while the coordinate of the 103.0 $cm^{-1}$ level is along the orthogonal direction. Surprisingly, it appears that the latter coordinate is similar to puckering. This situation will be reflected in the FC matrix and in the intensity distribution among the vibronic bands of emission and absorption spectrum.

In the following, we shall denote 39 and 38 as the modes of lower and higher frequency, respectively, both in $S_0$ and $S_1$.

In Table 3, we report also the $S_1$ vibrational energies proposed in ref 9. While the energies of the $39^n_0$ levels are in qualitative agreement with ours, the energies related to mode 38 are quite different. For example, the energies of the $38^1_0$, $38^2_0$, and $38^1_0$-$39^2_0$ levels are 189.5, 383.1, and 297.5 $cm^{-1}$, respectively, while the corresponding energies derived from our model are 103.0, 204.4, and 213.2 $cm^{-1}$, respectively. Furthermore, at variance with our results, the geometries of the minima in the two-dimensional $\tau$, $\phi$ PES found in ref 9 for the $S_0$ and $S_1$ states are roughly the same.

We have used the vibrational eigenfunctions obtained for the optimized potentials of $S_0$ and $S_1$ to compute the FC factors for the two large amplitude modes. These FC factors, which are reported in Tables 4 and 5, for the $a_1$ and $b_1$ states, respectively, govern the intensity distributions among the flapping and puckering vibrational bands observed in absorption and emission spectra. Therefore, they will be very helpful in analyzing the SVL fluorescence spectra[7] originating from a number of vibrational levels (vide infra). It can be seen that, as required by symmetry, a transition from a $b_1$ ($a_1$) level of $S_0$ will end at a $b_1$ ($a_1$) level of $S_1$.

It is worth noting that for any vibronic level of $S_0$ and $S_1$ the sum of the FC factors for the first seven levels does not sum up to 1. This is a consequence of the remarkable distortion of the $S_1$ PES with respect to the $S_0$ PES. Furthermore, FC factors between $38^n$ and $39_m$ levels are often larger than those between $39^n$ and $39_m$ or between $38^n$ and $38_m$ levels. An example is the large FC factor between the $S_1$ eigenvector assigned as $38^2_0$, at 204 $cm^{-1}$, and the $S_0$ eigenvector assigned as $39^0_2$, at 99 $cm^{-1}$,

**TABLE 4: Franck−Condon Factors for $a_1$ Puckering/ Flapping Vibrational Eigenstates of $S_0$ and $S_1$**

| $S_0\backslash S_1$ | 0.0[a] | 98.7[a] (102) | 150.0[a] (−)[b] | 204.4[a] (204) | 272.6[a] (271) | 297.6[a] (290) | 346.8[a] (354) | 408.9[a] (400) |
|---|---|---|---|---|---|---|---|---|
| 0.0[a] | 0.264 | 0.437 | <0.005 | 0.213 | 0.014 | 0.005 | 0.040 | <0.005 |
| 98.5[a] (99) | 0.074 | 0.057 | 0.234 | 0.314 | 0.134 | <0.005 | 0.096 | 0.039 |
| 236.0[a] (236) | 0.010 | <0.005 | 0.168 | <0.005 | <0.005 | 0.123 | 0.007 | 0.422 |
| 296.2[a] (299) | 0.068 | <0.005 | 0.123 | 0.102 | 0.005 | 0.256 | <0.005 | 0.225 |
| 403.9[a] (403) | 0.024 | <0.005 | 0.015 | 0.016 | 0.006 | <0.005 | 0.044 | 0.109 |
| 472.2[a] (472) | 0.025 | <0.005 | <0.005 | 0.020 | 0.012 | <0.005 | 0.037 | <0.005 |
| 545.8[a] (552) | 0.139 | <0.005 | <0.005 | <0.005 | 0.211 | 0.020 | 0.120 | 0.008 |
| 581.7[a] (583) | 0.030 | <0.005 | 0.020 | 0.022 | 0.030 | <0.005 | 0.036 | 0.023 |

[a] Computed wavenumbers ($cm^{-1}$) of vibrational levels. In parentheses are the inferred wavenumbers (Tables 2 and 3). [b] Not observed in the excitation spectrum.

**TABLE 5: Franck−Condon Factors for $b_1$ Puckering/ Flapping Vibrational Eigenstates of $S_0$ and $S_1$**

| $S_0\backslash S_1$ | 9.0[a] (−)[b] | 103.0[a] (102) | 185.1[a] (188) | 213.2[a] (197) | 270.8[a] (266) | 305.3[a] (310) | 364.7[a] (381) |
|---|---|---|---|---|---|---|---|
| 8.7[a] (8.66) | 0.124 | 0.516 | 0.064 | 0.185 | 0.07 | 0.040 | <0.005 |
| 156.8[a] (157) | 0.051 | 0.040 | 0.017 | 0.002 | 0.116 | 0.570 | 0.011 |
| 274.2[a] (278) | 0.151 | <0.005 | 0.286 | 0.016 | 0.246 | <0.005 | 0.109 |
| 324.5[a] (325) | 0.035 | <0.005 | 0.084 | 0.018 | 0.108 | <0.005 | 0.053 |
| 386.6[a] (388) | 0.013 | 0.021 | 0.074 | 0.048 | 0.065 | 0.093 | 0.078 |
| 489.7[a] (490) | 0.010 | 0.019 | 0.010 | 0.049 | 0.010 | 0.000 | <0.005 |
| 557.5[a] (−) | 0.066 | 0.026 | 0.006 | 0.055 | 0.014 | 0.008 | 0.000 |

[a] Computed wavenumbers ($cm^{-1}$) of vibrational states. In parentheses are the inferred wavenumbers (see Tables 2 and 3). [b] Not observed in the excitation spectrum.

while the FC factor between the $S_1$ eigenvector assigned as $38^2_0$, at 204 $cm^{-1}$, and the $S_0$ eigenvector assigned as $38^0_2$, at 552 $cm^{-1}$, is negligible. A second interesting example is the large FC factor between the $S_1$ eigenvector assigned as $38^1_0$, at 103 $cm^{-1}$, and the $S_0$ eigenvector assigned as $39^0_1$, at 8.7 $cm^{-1}$, while the FC factor between the $38^1_0$ eigenvector of $S_1$ and the $38^0_1$ eigenvector of $S_0$, at 278 $cm^{-1}$, is quite small. These observations reflect the rotation of the two large amplitude 38 and 39 coordinates upon excitation from $S_0$ and $S_1$.

A transition from a $b_1$ to an $a_1$ level could be observed only for a $b_1$ mode that borrows intensity from a higher $S_n(\sigma-\pi^*)$ state of the $b_1$ symmetry type. Following the Herzberg−Teller (HT) theory,[18,19] the borrowing is mediated predominantly by the $S_1-S_n$ vibronic coupling, which is typically of the order of 0.1 eV. In the case of BDO, the lowest electronic excited state $S_n(\sigma-\pi^*)$ of the $b_1$ symmetry type is 2.73 eV above $S_1$ and the $S_n(\sigma-\pi^*) \leftarrow S_0$ oscillator strength is 0.002 according to our CIS calculations. Thus, the borrowing of intensity from $S_n(\sigma-\pi^*) \leftarrow S_0$ to $S_1 \leftarrow S_0$ by $b_1$ vibrations is highly inefficient.

## 4. Analysis of IR and Fluorescence Excitation Spectra of BDO

**A. Assignment of Far IR Spectrum.** The far IR spectrum of BDO has been measured by Duckett et al.[2] and more recently by Sakurai et al.[6] The bands appearing in the 0−200 $cm^{-1}$ interval are due to transitions between vibrational levels of puckering and flapping motions. In this section, we analyze the IR spectrum of BDO vapor reported in ref 6 and qualitatively represented in Figure 5. We make use of the energies of the $S_0$ vibrational levels calculated in this work and displayed in Table 2, and we take into account also the comparison between the measured and calculated intensities.

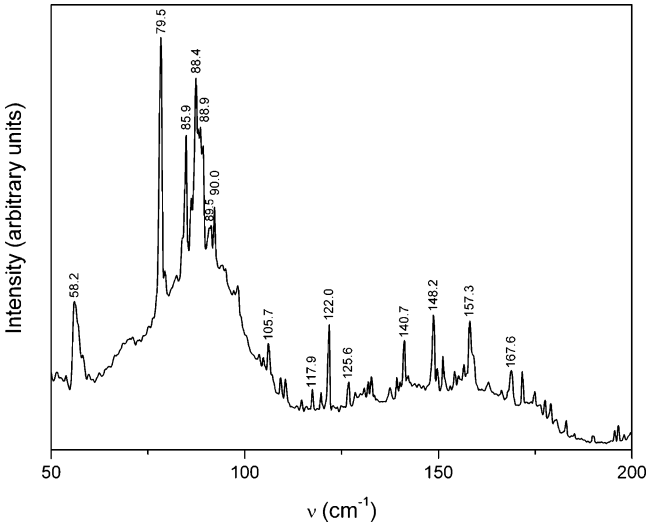


**Figure 5.** Far IR spectrum of BDO (adapted from ref 6).

We have modeled the IR band intensities by expressing the dependence of the $z$ and $x$ components of the dipole moment on the puckering ($\tau$) and flapping ($\phi$) motions by the relations

$$M_z(\tau, \phi) = M_0 \cos(\tau + \phi)$$

$$M_x(\tau, \phi) = M_0 \sin(\tau + \phi)$$

Transitions with the change of an even (odd) number of $b_1$ quanta are polarized along the $z$ ($x$) axis. We have reported in Table 6 the calculated energy gaps between the puckering and flapping vibrational levels reported in Table 2 and the intensity calculated for each transition. We correlate these data with the frequencies and intensities taken from Table 1 or from Figure 1 of ref 6. Finally, we present our assignments together with the attributions given in recent work.[6,12]

The calculated energy gaps and intensities appear to be in good agreement with the data of the IR spectrum. Our interpretation is mostly in agreement with the assignments of ref 6. The most notable difference pertains to $\nu_{38}$ to which we assign the value 278 $cm^{-1}$ because this value is the only one compatible with the fluorescence spectrum. Laane and coworkers[6] prefer the 267 $cm^{-1}$ value, which corresponds to an IR band which we assign to the $38_1 \leftarrow 39_1$ band. There are other less significant differences in the assignments involving higher energy levels. This is not surprising, since a univocal assignment of the puckering and flapping quanta in a given level is not always possible because of the anharmonicity of these oscillators.

We have tried to assign most of the bands observed in the 0−160 $cm^{-1}$ section of the far IR spectrum and a few prominent bands between 160 and 300 $cm^{-1}$. It is worth noting that the bands above 300 $cm^{-1}$ are subject to interactions with levels due to other $b_1$ vibrations (for example, $\nu_{37}$) and this complicates further the assignment.

In conclusion, the data presented in Table 6 indicate that the energies of the puckering/flapping vibrational levels that we have

**TABLE 6: Assignment of the BDO IR Transitions of Lower Frequencies ($cm^{-1}$) Involving Puckering/Flapping Levels**

| $n' \leftarrow n''$ [a] | assignment[a] $v_p', v_f' \leftarrow v_p'', v_f''$ | $\Delta E$ calcd[a] ($cm^{-1}$) | $I$ rel.[a] | $\Delta E$ inferred[a] ($cm^{-1}$) | IR[b] | assignment[c] $v_p' \leftarrow v_p''$ | assignment[b] |
|---|---|---|---|---|---|---|---|
| 3 ← 2 | 3,0 ← 2,0 | 58.3 | 0.58 | 57 | 58.2 s | 3 ← 2 | 3,0 ← 2,0 |
| 6 ← 4 | 1,1 ← 4,0 | 60.2 | <0.01 | 63 | 60.1 w | | 1,1 ← 4,0 |
| 4 ← 3 | 4,0 ← 3,0 | 79.2 | 0.81 | 80 | 79.5 s | 2 ← 1 | 4,0 ← 3,0 |
| 9 ← 7 | 6,0 ← 5,0 | 79.4 | 0.39 | 78 | 80.0* mw | | - |
| 10 ← 8 | 3,1 ← 2,1 | 85.5 | 0.28 | 84 | 85.9 m | 5 ← 4 | 2,1 ← 1,1 |
| 11 ← 9 | 4,1 ← 6,0 | 85.9 | 0.34 | 87 | 88.9 ms | | 3,1 ← 2,1 |
| 7 ← 4 | 5,0 ← 4,0 | 88.5 | 0.65 | 89 | 88.4 s | 4 ← 3 | 5,0 ← 4,0 |
| 2 ← 1 | 2,0 ← 1,0 | 89.9 | 0.82 | 90 | 89.5 s | - | 2,0 ← 1,0 |
| 8 ← 6 | 2,1 ← 1,1 | 90.4 | 0.31 | 89 | 90.0 ms | | 6,0 ← 5,0 |
| 2 ← 0 | 2,0 ← 0,0 | 98.5 | 0.05 | 99 | 98.8 vw | | 2,0 ← 0,0 |
| 9 ← 6 | 6,0 ← 1,1 | 107.7 | <0.01 | 104 | 105.7* w | | - |
| 8 ← 5 | 2,1 ← 0,1 | 112.4 | 0.01 | 109 | 109.9 w | | 0,1 ← 3,0 |
| 5 ← 3 | 0,1 ← 3,0 | 117.4 | <0.01 | 121 | 117.9 mw | | 6,0 ← 1,1 |
| 15 ← 10 | - | 120.4 | 0.23 | | 122.0* ms | | - |
| 9 ← 5 | 2,1 ← 0,1 | 129.7 | 0.10 | 125 | 125.6* m | | - |
| 4 ← 2 | 4,0 ← 2,0 | 137.5 | 0.07 | 137 | 137.2 mw | | 4,0 ← 2,0 |
| 6 ← 3 | 1,1 ← 3,0 | 139.4 | 0.20 | 143 | 140.7 s | | 1,1 ← 3,0 |
| 10 ← 7 | 3,1 ← 5,0 | 147.7 | 0.20 | 147 | 149.1* mw | | - |
| 3 ← 1 | 3,0 ← 1,0 | 148.1 | 0.11 | 147 | 148.2 s | 3 ← 0 | 3,0 ← 1,0 |
| 8 ← 4 | 2,1 ← 4,0 | 150.6 | 0.10 | 152 | 151.3* mw | | - |
| 3 ← 0 | 3,0 ← 0,0 | 156.8 | 0.44 | 156 | 157.3 vs | | 3,0 ← 0,0 |
| 7 ← 3 | 5,0 ← 3,0 | 167.7 | 0.10 | 168 | 167.6 ms | | 5,0 ← 3,0 |
| 5 ← 2 | 0,1 ← 2,0 | 177.7 | 0.03 | 179 | 178.7 w | | 6,0 ← 4,0 |
| 6 ← 2 | 1,1 ← 2,0 | 197.7 | 0.02 | 200 | 198.7 w | | 1,1 ← 2,0 |
| 4 ← 1 | 4,0 ← 1,0 | 227.3 | 0.10 | 227 | 227.8 s | 4 ← 1 | 4,0 ← 1,0 |
| 7 ← 2 | 5,0 ← 2,0 | 226.0 | 0.12 | 226 | | | |
| 4 ← 0 | 4,0 ← 0,0 | 236.0 | 0.04 | 236 | 236.4 m | 5 ← 2 | 4,0 ← 0,0 |
| 5 ← 1 | 0,1 ← 1,0 | 265.7 | 0.00 | 269 | 267.2 mw | | 0,1 ← 0,0 |
| 6 ← 0 | 1,1 ← 0,0 | 296.2 | 0.01 | 299 | 297.8 m | | 1,1 ← 0,0 |

[a] This work, frequencies and assignment from Table 2. [b] From ref 6, frequencies with asterisk were read on the spectrum. [c] From ref 12.

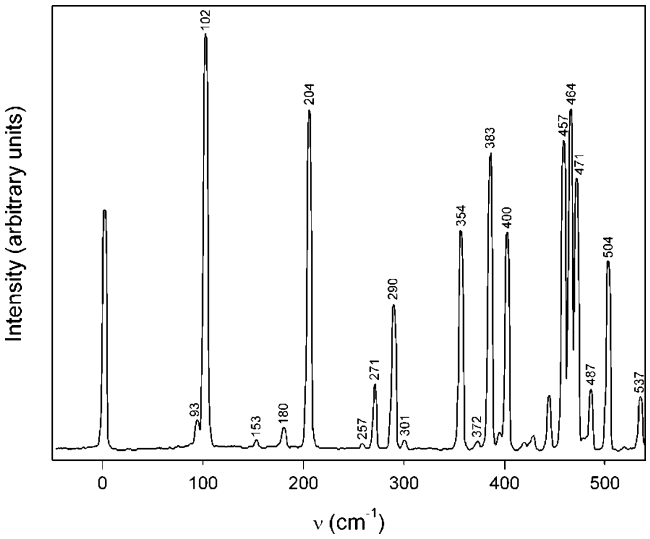


**Figure 6.** Excitation spectrum of BDO in supersonic beam (adapted from ref 9).

obtained by means of the CASPT2 calculations are reliable. All together, this provides strong support for the $S_0$ PES obtained by us and for the 125.7 $cm^{-1}$ estimate for barrier height, a value which is slightly lower than the value suggested by Laane and co-workers[6] but almost identical to the value found earlier by Caminati and co-workers.[5] A further check to these assignments will be provided by the analysis of SVL spectra (vide infra).

**B. Assignment of the Fluorescence Excitation Spectrum in Supersonic Beams.** The vibrational levels reported in Table 3 allow us to provide the assignment of a number of bands observed in the BDO excitation spectrum measured in supersonic beams,[9] which is qualitatively represented in Figure 6. The assignments of the vibronic bands of this spectrum are summarized in Table 7 where we quote also the assignments proposed earlier.[9]

Before analyzing the excitation spectrum in detail, we recall that the $S_1 \leftarrow S_0$ transition is of appreciable intensity and the ability of $b_1$ vibrations to induce $S_1 \leftarrow S_0$ intensity by the HT mechanism is negligible. Therefore, the vibronic bands with appreciable intensity in the allowed $S_1 \leftarrow S_0$ transition are the ones associated with considerable FC factors.

Besides the 0−0 band, the lowest-energy bands of appreciable intensity in the excitation spectrum of BDO are the hot band at 93 $cm^{-1}$ and the cold band at 104 $cm^{-1}$. From the calculated levels shown in Table 3 and from the FC factors reported in Tables 4 and 5, the obvious assignments for the two bands are $39^0_1 38^1_0$ and $39^2_0$, respectively. In ref 9, it is proposed that the 93 $cm^{-1}$ band is assigned to the $39^2_1$ transition. In our view, this assignment is very unlikely because it is confronted with a zero FC factor. Moreover, recently, Pietraperzia et al.[12] by studying rotational contours have shown that this band cannot be associated with a transition having the same final vibronic level as the 104 $cm^{-1}$ band.

Surprisingly, no band in the excitation spectrum can be assigned with confidence as $39^1_1$. In fact, no band of appreciable intensity is observed in the spectral region from −10 to +50 $cm^{-1}$ with respect to the origin. Since the $\nu_{39}$ fundamental in $S_0$ is 8.67 $cm^{-1}$ [12] and according to the present CASPT2 PES of $S_1$ the $\nu_{39}$ fundamental is 21.5 $cm^{-1}$ (see Tables 3 and 7), we expect that the $39^1_1$ band should be found approximately between the origin and 20 $cm^{-1}$ above the origin. The calculated FC factors (see Table 5) indicate that the intensity of the $39^1_1$ band is about 25% of the intensity of the $39^0_1 38^1_0$ band observed at 93 $cm^{-1}$. Since in the excitation spectrum[9] the intensity of the latter is about 10% of the intensity of the origin band, the intensity of the $39^1_1$ band should be roughly 2.5% of the intensity of the origin band. Therefore, the $39^1_1$ band could be

**TABLE 7: Assignment of Vibrational Bands in the $S_1-S_0$ Excitation Spectrum**

| excitation spectrum bands[a] ($cm^{-1}$) | inferred frequencies[b] ($cm^{-1}$) | excitation bands from optimized PES[c] | assignment of observed bands (present work) | assignment of observed bands (from ref 9) |
|---|---|---|---|---|
| −14 H | | −14[d] | $20^1_1$; $20^1_1 39^1_1$ | $20^1_1$ |
| 0 | | 0 | 0−0 | 0−0 |
| <1 H | 10 | <1 | $39^1_1$ | $39^1_1$ |
| 54 H | | 51.5; 61.6 | $39^1_2 38^1_0$; $39^2_4 38^2_0$ | |
| 93 H | 102 | 94 | $39^0_1 38^1_0$ | $39^1_2$ |
| 102 G | 102 | 99 | $39^2_0$ | $39^2_0$ |
| | | 150 | $39^1_0 38^1_0$ | |
| 153 H | | 149 | $39^0_3 38^3_0$ | $39^3_1$ |
| 180 H | 188 | 176 | $39^3_1$ | $39^0_1 38^1_0$ |
| 189 H | 197 | 204 | $39^2_1 38^1_0$ | $38^1_0$ |
| 204 G | 204 | 204 | $38^2_0$ | $39^1_0 38^1_0$ |
| 257 H | 266 | 262 | $39^1_1 38^2_0$ | $37^1_0 39^2_1$ |
| 271 G | 271 | 273 | $39^4_0$ | $39^4_0$ |
| 290 G | 290 | 298 | $39^3_0 38^1_0$ | $39^2_1 38^1_0$ |
| 301 H | 310 | 296 | $38^3_0 39^0_1$ | $39^3_2 38^1_0$ |
| 354 G | 354 | 347 | $39^2_0 38^2_0$ | $37^1_0 39^1_0$ |
| 372 H | 381 | 356 | $39^5_1$ | $39^5_1$ |
| 383 G | | 371[d] | $37^1_0 38^1_0$ | $38^2_0$ |
| 400 G | 400 | 409 | $38^4_0$; $39^1_0 38^3_0$ | $39^3_0 38^1_0$ |
| 457 G | 457 | 473[d,e] | $39^2_0 38^1_0 37^1_0$ | |
| 464 G | 464 | 464[d] | $14^1_0$ | |

[a] From ref 9; G and H indicate cold and hot bands, respectively. [b] From observed bands, by adding an energy of 8.66 $cm^{-1}$ to the frequencies of hot bands originating from the level $39^0_1$ of the ground state. [c] See text and Table 3. [d] From the data of Tables 2 and 3. [e] From $\nu_{37} = 269$ and $39^2_1 38^1_0 = 204$ $cm^{-1}$.

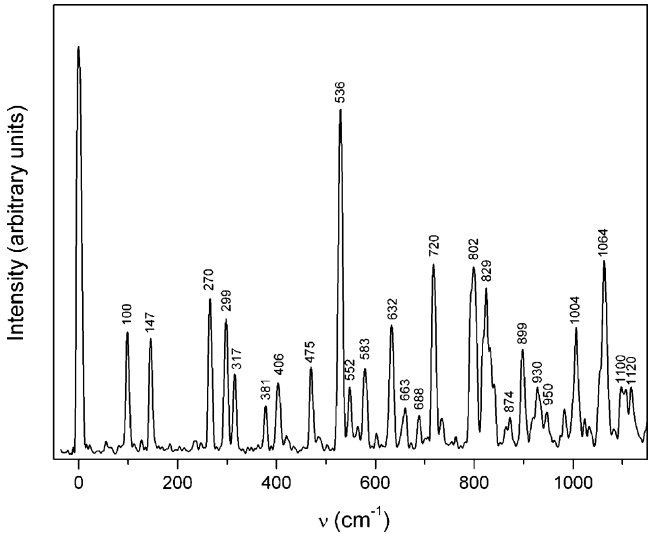


**Figure 7.** SVL spectrum following the excitation of the origin band (adapted from ref 7).

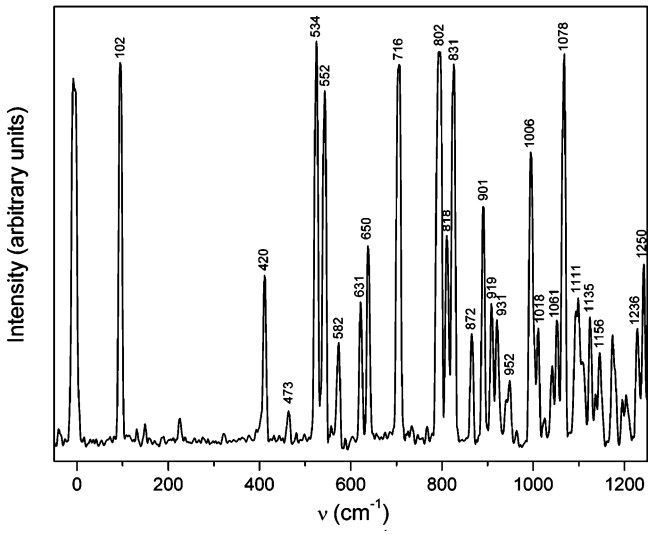


**Figure 8.** SVL spectrum following the excitation of the 102 $cm^{-1}$ band (adapted from ref 7). Frequencies on the top of the bands were read on the spectrum.

observed if it were distinct from the origin band but could go easily unnoticed if it were buried under it. The suggestion that the $39^1_1$ transition should correspond to the hot band observed 1.4 $cm^{-1}$ above the origin[9] was recently shown[12] to not be compatible with the rotational contour of the band. Therefore, we propose that the $39^1_1$ transition falls within the origin band and that it was so far unnoticed because of its comparatively weak intensity. A strong support for this proposal is provided by the vibronic structure of the SVL fluorescence emitted from the origin band (vide infra).

Above 104 $cm^{-1}$, the next bands with appreciable intensity are the hot band at 180 $cm^{-1}$ and the very strong and cold band at 204 $cm^{-1}$. Following Table 7, we assign these two bands as $39^3_1$ and $38^2_0$, respectively. These assignments suggest that in state $S_1$ mode 38 behaves roughly as a harmonic mode with a frequency of ~100 $cm^{-1}$ and that mode 39 behaves in a similar way as in $S_0$, although with a slightly higher frequency.

At higher energies, we find in the BDO excitation spectrum three cold bands of medium−strong or strong intensities at 271, 290, and 354 $cm^{-1}$. According to our calculations, these bands can be assigned as $39^m_0 38^n_0$, with $m + n = 4$.

The hot and rather weak bands observed at 189, 257, 301, and 372 $cm^{-1}$ are all assigned to transitions originating from the $39_1$ vibronic level of $S_0$. In particular, we assign them as $39^2_1 38^1_0$, $39^1_1 38^2_0$, $39^0_1 38^3_0$, and $39^5_1$, respectively.

The cold band detected at 400 $cm^{-1}$ is assigned as $38^4_0$. The other cold bands in this region, namely, the 383, 457, and 464 $cm^{-1}$ bands, are assigned to other modes, either to combination bands with $\nu_{39}$ or to the $a_1$ mode $\nu_{14}$, as indicated in Table 7. We shall discuss the assignments of these bands below when we consider the corresponding SVL spectra.

Some of the hot bands identified in the excitation spectrum are due to transitions originating from vibrational levels of $S_0$ different than the $39_1$ vibronic level. We assign the hot band observed at −14 $cm^{-1}$ to the overlapping $20^1_1$ and $20^1_1 39^1_1$ transitions because of the vibronic structure of the corresponding SVL spectrum. In previous work, this band was attributed to

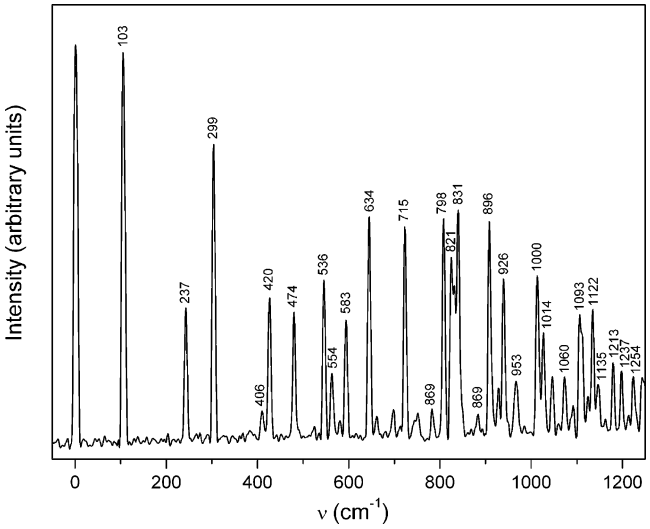


**Figure 9.** SVL spectrum following the excitation of the 204 $cm^{-1}$ band (adapted from ref 7). Frequencies on the top of the bands were read on the spectrum.

the $20^1_1$ transition,[9] while, more recently, $20^1_1 39^2_2$ was considered to be a preferable choice on the basis of the rotational contour of this band.[12] Furthermore, as indicated in Table 7, we assign the weak hot bands at 54 and 153 $cm^{-1}$ to $39^2_4 38^2_0$ and as $39^0_3 38^3_0$, respectively.

Interestingly, the transition $39^1_0 38^1_0$ calculated with an energy of 150 $cm^{-1}$ and with practically zero intensity is not observed in the excitation spectrum.

Comparing our interpretation with the assignments of the excitation spectrum proposed in ref 9, it appears that the analogies are fewer than the discrepancies. This is the expected consequence of the differences in the $S_1$ PES noted above.

**C. SVL Fluorescence Spectra in Supersonic Beams.** The SVL fluorescence spectra are a powerful means to test the assignment of the bands in the excitation spectrum.

Hassan and Hollas,[4] who were the first to record SVL fluorescence spectra of BDO seeded in supersonic beams, reported the spectra emitted from three bands, namely, the $S_1$ origin and the $S_1 + 102$ $cm^{-1}$ and $S_1 + 204$ $cm^{-1}$ bands. More recently, Sakurai has measured[7] the SVL fluorescence spectra emitted from about 10 vibronic levels of $S_1$, including the ones reported in ref 4. The spectra of the latter author cover the interval 0−1100 $cm^{-1}$, while the spectra of the former authors extend from 0 to about 2000 $cm^{-1}$. Since we are interested in the assignment of the bands associated with the puckering and flapping modes, we are concerned with the bands in the 0−580 $cm^{-1}$ section of the fluorescence spectrum.

We begin by discussing the three SVL spectra emitted from the origin, the 102 $cm^{-1}$ band, and the 204 $cm^{-1}$ band of the excitation spectrum, which are shown in Figures 7, 8, and 9, respectively. The assignments of these spectra are presented in Table 8. A group of frequencies, namely, 100, 236, 299, 403, 474, 536, 552, and 583 $cm^{-1}$, appear in all three spectra of both authors. With the exception of the band at 536 $cm^{-1}$, which is associated with $\nu_{14}$, the lowest $a_1$ frequency, all of the other bands result from transition to $S_0$ vibronic levels with an even number of $\nu_{38}$ and $\nu_{39}$ quanta. This fluorescence structure is the one we expect for the emission from the $S_1$ origin. The fact that also the fluorescence spectra from the $S_1 + 102$ $cm^{-1}$ and $S_1 + 204$ $cm^{-1}$ bands show a vibrational structure based on bands of the same $a_1$ total symmetry indicates that also these two bands are of type $a_1$. This is compatible with the assignments proposed in Table 3 where the $S_1 + 102$ $cm^{-1}$ and $S_1 + 204$ $cm^{-1}$ bands are assigned as $39_0^2$ and $38_0^2$, respectively.

Let us consider the intensities of the even-quanta bands in the three spectra. The observed fluorescence intensities parallel qualitatively the trends of the calculated FC factors associated with the three emitting levels, namely, the origin, +102 $cm^{-1}$, and +204 $cm^{-1}$ (see Table 4). In particular, the fluorescence band at 236 $cm^{-1}$ is weak, is absent, and has a medium−strong intensity in the SVL emission from the origin, the 102 $cm^{-1}$ band, and the 204 $cm^{-1}$ band, respectively. The bands at 99 and 299 $cm^{-1}$ are absent in the SVL spectrum from the 102 $cm^{-1}$ band but are strong in the other two SVL spectra.

By considering the SVL fluorescence from the origin reported in refs 6 and 7 and shown in Figure 7, we notice with surprise that also levels due to an odd number of $\nu_{38}$ and $\nu_{39}$ quanta appear in the spectrum. Among these, we notice bands at 147 $cm^{-1}$ ($39^1_3$), 270 $cm^{-1}$ ($39^1_0 38^0_1$), 317 $cm^{-1}$ ($39^1_5$), and 381 $cm^{-1}$ ($39^1_2 38^0_1$). The presence of these bands indicates that, by exciting the molecule with the laser light aimed at the 0−0 transition, one excites both the cold 0−0 and the hot $39^1_1$ transitions. The level $39_1$ can be easily populated also in a cold beam of 5−10 K because of its low energy (8.66 $cm^{-1}$). It is worth noting that in the SVL spectrum emitted by the origin band reported by Hassan and Hollas[4] the bands corresponding to odd numbers of $\nu_{38}$ and $\nu_{39}$ quanta are absent. This observation implies that the puckering frequency has similar values, close to 9 $cm^{-1}$, in both electronic states and that the $39^1_1$ band lies within the 0−0 band but spans only a fraction of it. In this way, one may account for the fact that, in different

**TABLE 8: SVL Fluorescence Spectra ($cm^{-1}$) of BDO Emitted from the 0−0, $39^2_0$, and $39^4_0$ Vibronic Levels of $S_1$ (the Energy of the Origin Is 34 788 $cm^{-1}$)**

| $(0_0^0)$;[a,c] $39^1_1$ | assignment | (0−0)[b] | $39^2_0$[a] (102 $cm^{-1}$) | assignment | $38^2_0$[a] (204 $cm^{-1}$) | assignment |
|---|---|---|---|---|---|---|
| 0 vs | 0−0 | 0 vs | 0 vs | $39^2_0$ | 0 vs | $38^2_0$ |
| 100 s | $39^0_2$ | 99 s | 102 vs | $39^2_2$ | 103 vs | $39^0_2 38^2_0$ |
| *147 s* | $39^1_3$ | | | | | |
| 236 vw | $39^0_4$ | 233 vw | | | 237 ms | $39^0_4 38^2_0$ |
| *270 s* | $39^1_0 38^0_1$ | | | | | |
| 299 s | $39^0_1 38^0_1$ | 299 ms | | | 299 vs | $39^0_1 38^2_1$ |
| *317 m* | $39^1_5$ | | | | | |
| *381* mw | $39^1_2 38^0_1$ | | | | | |
| 406 m | $39^0_3 38^0_1$ | 403 m | | | 406 w | $39^0_3 38^2_1$ |
| | $39^0_1 37^0_1$ | | 420 ms | $39^2_1 37^0_1$ | 420 ms | $39^0_1 38^2_0 37^0_1$ |
| 475 m | $39^0_6$ | 472 m | 473 w | $39^2_6$ | 474 ms | $39^0_6 38^2_0$ |
| 536 vs | $14^0_1$ | 535 vs | 534 vs | $39^2_0 14^0_1$ | 536 ms | $38^2_0 14^0_1$ |
| 552 mw | $38^0_2$ | 550 mw | 552 vs | $39^2_0 38^0_2$ | 554 m | $38^2_2$ |
| 572 | $39^0_3 37^0_1$ | | | | | |
| 583 m | $39^0_5 38^0_1$ | 580 m | 582 m | $39^2_5 38^0_1$ | 583 m | $39^0_5 38^2_1$ |

[a] From refs 6 and 7. [b] From ref 4. [c] Energies of $b_1$-type levels are in italics.

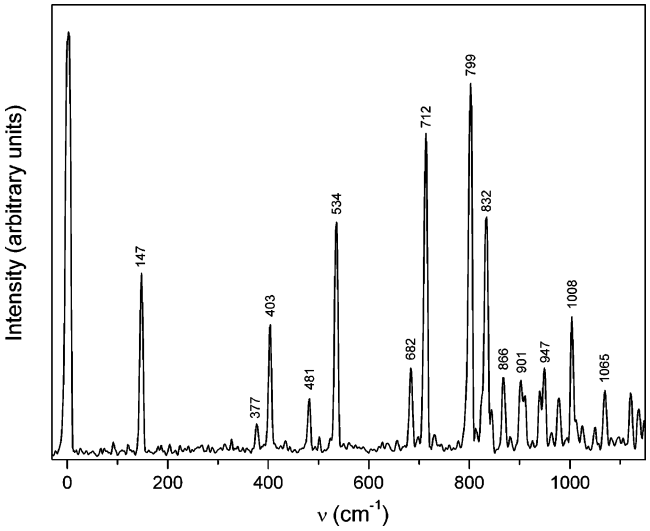


**Figure 10.** SVL spectrum following the excitation of the 93 $cm^{-1}$ band (adapted from ref 7). Frequencies on the top of the bands were read on the spectrum.

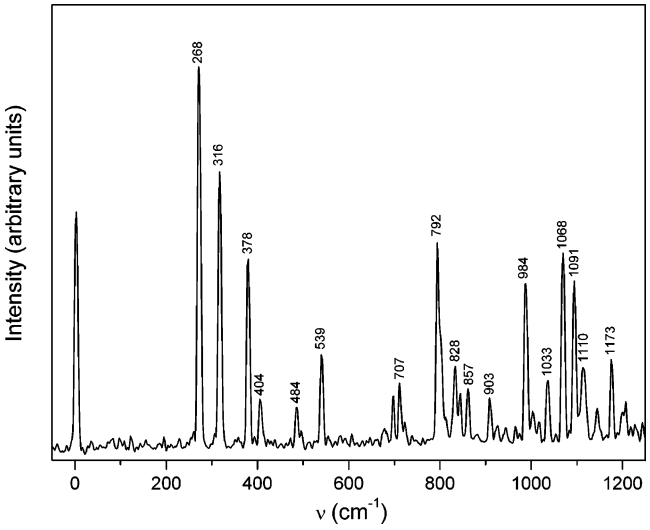


**Figure 11.** SVL spectrum following the excitation of the 180 $cm^{-1}$ band (adapted from ref 7). Frequencies on the top of the bands were read on the spectrum.

experiments, the excitation of the origin band may or may not produce also the excitation of the $39^1_1$ band.

We discuss next the structure of SVL spectra originating from the hot excitation bands at 93 and 180 $cm^{-1}$, which are reported in ref 7. The assignments of these spectra, which are shown in Figures 10 and 11, are given in Table 9. The SVL fluorescence spectra emitted from these two bands contain only odd numbers of $b_1$ quanta. This observation, which implies that the emitting levels are of the $b_1$ type, is in agreement with the assignment of these two excitation bands as $39^0_138^1_0$ and $39^2_138^1_0$, respectively, proposed in the previous section. The intensity distribution among the puckering and flapping vibronic levels in the two fluorescence spectra correlates well with the FC factors reported in Table 5. This applies in particular to the strong band observed at 148 $cm^{-1}$ in the SVL fluorescence emitted from the $39^0_138^1_0$ band and to the strong emissions at 271, 316, and 378 $cm^{-1}$ in the SVL spectrum from the $39^2_1$-$38^1_0$ band. The previous assignment[9] of the excitation band at 93 $cm^{-1}$ to the $39^2_1$ transition is incompatible with the vibronic structure of the fluorescence spectrum and was criticized[12] also on the basis of the rotational structure of this band.

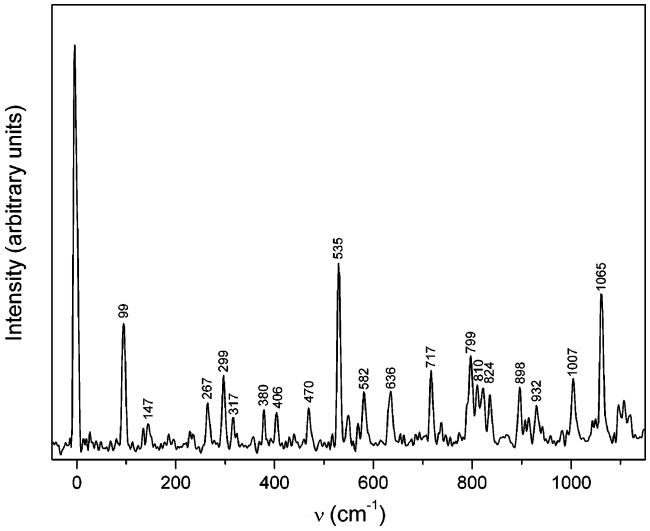


**Figure 12.** SVL spectrum following the excitation of the −14 $cm^{-1}$ band (adapted from ref 7). Frequencies on the top of the bands were read on the spectrum.

The assignments of SVL spectra originating from the excitation bands at −14, 290, 383, and 464 $cm^{-1}$, reported in ref 7, are given in Table 10. The assignment of the hot band observed at −14 $cm^{-1}$ as $20^1_1$ is compatible with the values of the $\nu_{20}$ frequencies in $S_0$ and $S_1$.[9] The SVL fluorescence spectrum emitted from this band, shown in Figure 12, is dominated by bands of $a_1$ nature and of even numbers of $b_1$ quanta. However, we notice also weak bands at 147, 267, and 317 $cm^{-1}$ involving odd numbers of $b_1$ quanta. This observation suggests that the hot band at −14 $cm^{-1}$ comprises both the $20^1_1$ and $20^1_139^1_1$ bands. This fact provides further support to the idea that the $39^1_1$ band coincides with the origin band.

The excitation of the bands at 290 and 383 $cm^{-1}$ leads to SVL fluorescence spectra that include bands corresponding to even numbers of $b_1$ quanta in $S_0$. It follows that the two bands are all of $a_1$ total symmetry. This conclusion agrees and supports their assignment as $39^2_038^2_0$, $37^1_038^1_0$, respectively, proposed in Table 3 by considering the $S_1$ vibronic levels. The large intensity of the 297 $cm^{-1}$ band and the weakness of the 98 $cm^{-1}$ band in the SVL spectrum emitted from the excited 290 $cm^{-1}$ band is in agreement with the FC factors shown in Table 4. At the same time, the large intensities observed for the bands at 401 and 419 $cm^{-1}$ in the SVL spectrum emitted from the excited 383 $cm^{-1}$ band agrees with the involvement of $\nu_{37}$ in this excitation band.

The 464 $cm^{-1}$ band in the excitation spectrum is attributed to the $14^1_0$ transition (vide supra). This assignment is supported by considering the relevant SVL fluorescence spectrum, in particular by the observation that the intensity of the 1058 $cm^{-1}$ band observed in and attributed to $2\nu_{14}$ is even larger than the intensity of the $\nu_{14}$ band. This intensity trend reflects the usual features of the FC factors pertinent to transitions from a vibronic state with $v = 1$.[20]

We consider next the structures of SVL spectra originating from the bands at 271, 354, 400, and 301 $cm^{-1}$ of the excitation spectrum. These SVL spectra to our knowledge have not been measured and reported yet. We show in Table 11 the qualitative structure of these spectra predicted on the basis of the calculated FC factors reported in Tables 4 and 5. The fluorescence spectrum emitted from the 271, 354 $cm^{-1}$ excitation bands are both expected to be dominated by the 100 $cm^{-1}$ band. The excitation band at 400 $cm^{-1}$ is predicted to emit a SVL spectrum with intense bands at 236, 299, and 403 $cm^{-1}$. The hot band

**TABLE 9: Assignments of the SVL Fluorescence Spectra ($cm^{-1}$) of BDO Emitted from the $39_1 38^1_0$ and $39^2_1 38^1_0$ Vibronic Levels of $S_1$ (for Comparison, the Fluorescence from the Origin and the $39^1_1$ Level Is Reported)**

| $(0_0^0)$;[a,c] $39^1_1$ | assignment | $39^0_1 38^1_0$[b] ($93\ cm^{-1}$) | assignment | $39^2_1 38^1_0$[b] ($180\ cm^{-1}$) | assignment |
|---|---|---|---|---|---|
| 0 vs | $0-0$; $39^1_1$ | 0 vs | $39^0_1 38^1_0$ | 0 vs | $39^2_1 38^1_0$ |
| 100 s | $39^0_2$ | | | | |
| *147 s* | $39^1_3$ | 148 s | $39^0_3 38^1_0$ | | |
| 236 vw | $39^0_4$ | | | | |
| *270 s* | $39^1_0 38^0_1$ | | | 271 vs | $39^2_1 38^1_1$ |
| 299 s | $39^0_1 38^0_1$ | | | | |
| *317 m* | $39^1_5$ | | | 316 vs | $39^2_5 38^1_0$ |
| *381* mw | $39^1_2 38^0_1$ | 377 vw | $39^0_2 38^1_1$ | 378 s | $39^2_2 38^1_1$ |
| 406 m | $39^0_3 38^0_1$ | | | | |
| | | 404 ms | $38^1_0 37^0_1$ | 403 w | $39^2_0 38^1_0 37^0_1$ |
| | $39^0_1 37^0_1$ | | | | |
| 475 m | $39^0_6$ | | | | |
| | | 481 w | $39^0_4 38^1_1$ | 482 w | $39^2_4 38^1_1$ |
| 536 vs | $14^0_1$ | 534 s | $39^0_1 38^1_0 14^0_1$ | 536 m | $9^2_1 38^1_0 14^0_1$ |
| 552 mw | $38^0_2$ | | | | |

[a] From refs 6 and 7. [b] From ref 7. [c] Energies of $b_1$-type levels are in italics.

**TABLE 10: Assignment of the SVL Fluorescence Spectra ($cm^{-1}$) of BDO Emitted from the $20^1_1$, $39^2_0 38^2_0$, $37^1_0 38^1_0$, and $14^1_0$ Vibronic Levels of $S_1$[a]**

| $20^1_1$; $20^1_1 39^1_1$ ($-14\ cm^{-1}$) | assignment | $39^2_0 38^2_0$ ($290\ cm^{-1}$) | assignment | $37^1_0 38^1_0$ ($383\ cm^{-1}$) | assignment | $14^1_0$ ($464\ cm^{-1}$) | assignment |
|---|---|---|---|---|---|---|---|
| 0 s | $20^1_1$ | 0 s | $39^2_0 38^2_0$ | 0 vs | $37^1_0 38^1_0$ | 0 s | $14^1_0$ |
| 99 ms | $20^1_1\ 39^0_2$ | 98 mw | $39^2_2 38^2_0$ | 98 w | $37^1_0 38^1_0 39^0_2$ | 98 ms | $14^1_0 39^0_2$ |
| *147* w | $20^1_1\ 39^1_3$ | | | | | | |
| | | 237 m | $39^2_4 38^2_0$ | | | | |
| *267* w | $20^1_1\ 39^1_0 38^0_1$ | | | | | | |
| 299 mw | $20^1_1\ 39^0_1 38^0_1$ | 297 vs | $39^2_1 38^2_1$ | 298 ms | $37^1_0 38^1_1 39^0_1$ | | |
| *317* w | $20^1_1\ 39^1_5$ | | | | | | |
| *380* w | $20^1_1\ 39^1_2 38^0_1$ | | | | | | |
| 406 w | $39^0_3 38^0_1$ | 401 m | $39^2_3 38^2_1$ | 401 vs | $37^1_0 38^1_1 39^0_3$ | | |
| | | 417 m | $39^2_1 38^2_0 37^0_1$ | 419 vs | $37^1_1 38^1_0 39^0_1$ | | |
| 470 w | $20^1_1 39^0_6$ | | | 468 w | $37^1_0 38^1_0 39^0_6$ | | |
| 535 s | $20^1_1 14^0_1$ | 532 s | $39^2_0 38^2_0 14^1_0$ | 530 mw | $37^1_0 38^1_0 14^1_0$ | 532 s | $14^1_1$ |
| | | 551 ms | $39^2_0 38^2_2$ | | | 549 s | $14^1_0 38^0_2$ |
| | | 568 ms | $39^2_3 38^2_0 37^0_1$ | 564 s | $37^1_1 38^1_0 39^0_3$ | | |
| 582 w | $20^1_1 39^0_5 38^0_1$ | | | 580 m | $37^1_0 38^1_1 39^0_5$ | | |
| | | | | | | 1058 vs | $14^1_2$ |

[a] From ref 7.

**TABLE 11: Predicted Vibronic Structure of Some SVL Fluorescence Spectra Not Measured Yet**

| $39^4_0$ ($271\ cm^{-1}$) | assignment | $39^1_0 38^3_0$ ($354\ cm^{-1}$) | assignment | $38^4_0$ ($400\ cm^{-1}$) | assignment | $39^0_1 38^3_0$ ($301\ cm^{-1}$) | assignment |
|---|---|---|---|---|---|---|---|
| 0 ms | $39^4_0$ | 0 ms | $39^1_0 38^3_0$ | 0 mw | $38^4_0$ | 0 m | $39^0_1 38^3_0$ |
| 100 vs | $39^4_2$ | 100 s | $39^1_2 38^3_0$ | 100 ms | $39^0_2 38^4_0$ | | |
| | | | | | | 148 vs | $39^0_3 38^3_0$ |
| | | 236 w | $39^1_4 38^3_0$ | 236 vs | $39^0_4 38^4_0$ | | |
| | | | | | | 271 w | $39^0_0 38^3_1$ |
| 299 mw | $39^4_1 38^0_1$ | | | 299 s | $39^0_1 38^4_1$ | | |
| | | | | | | 316 vs | $39^0_5 38^3_0$ |
| | | | | 377 vw | $39^1_2 38^4_1$ | 381 m | $39^0_2 38^3_1$ |
| 403 mw | $39^4_3 38^0_1$ | 403 ms | $39^1_3 38^3_1$ | 403 s | $39^0_3 38^4_1$ | | |
| | | | | | | 403 w | $39^0_0 38^3_0 37^0_1$ |
| | | 474 ms | $39^1_6 38^3_0$ | | | | |
| | | | | | | 482 w | $39^0_4 38^3_1$ |
| 554 vs | $39^4_0 38^0_2$ | | | | | | |
| 583 ms | $39^4_5 38^0_1$ | | | 583 ms | $39^0_5 38^4_1$ | | |

observed at $301\ cm^{-1}$ is expected to lead to a fluorescence spectrum with intense bands at 148 and $316\ cm^{-1}$. We hope that the corresponding SVL spectra will soon be available to test our results.

## 5. Conclusions

By accurate CASPT2 calculations of the $S_0$ and $S_1$ two-dimensional PES along the puckering ($\tau$) and flapping ($\phi$) coordinates, we have obtained a detailed description of the corresponding vibrational levels in both electronic states of BDO. The two potential energy surfaces show a planar barrier in both states, which we have determined to be $125.7\ cm^{-1}$ in $S_0$ and $190.4\ cm^{-1}$ in $S_1$. While in $S_0$ the two minima are found along the $\tau$ coordinate, in $S_1$ they require distortions of both coordinates. As a consequence of this effect as well as of the lowering of the flapping frequency in $S_1$, the two $S_1$ vibrational modes in the $\tau, \phi$ space are a linear combination of the two corresponding modes in $S_0$. That is, BDO offers a remarkable

Duschinsky effect. This fact makes it dangerous to attempt the interpretation of the vibronic structure of $S_0-S_1$ transitions on a simple intuitive basis.

On the basis of calculated $S_0$ vibrational levels, we could give a satisfactory interpretation of the far IR spectrum of BDO. We have provided an assignment of the excitation spectrum that is supported by the consistent interpretation of the SVL fluorescence spectra emitted by a number of bands of the excitation spectrum.

The ability to successfully assign the $S_0$ and $S_1$ spectra suggests that the derived $S_0$ and $S_1$ PES are correct. In particular, it supports the estimates of the planar barrier heights in both states outlined above.

The barrier to planarity increases from 125.7 $cm^{-1}$ in $S_0$ to 190.4 $cm^{-1}$ in $S_1$. We attribute this effect to the reduced rigidity in the excited state that is attested by the decrease of the quadratic coefficient of the flapping potential upon excitation (from 4.797 $cm^{-1}$ $deg^{-2}$ in $S_0$ to 0.505 $cm^{-1}$ $deg^{-2}$ in $S_1$). This decrease may be related to the change of the benzene $\pi$-system/oxygen lone pair interaction with the excitation: it is of van der Waals type in $S_0$ and of exciplex type in $S_1$. Thus, the molecule distorted along the flapping coordinate is stabilized more in $S_1$ than in $S_0$.

**Acknowledgment.** We are indebted to Prof. J. Laane for sending us a copy of the Sakurai thesis and to Prof. W. Caminati for many stimulating discussions. The financial support from MIUR (project, "Modellistica delle Proprietà Spettroscopiche di Sistemi Molecolari Complessi" funds ex 60%; project, "Dinamiche Molecolari in Sistemi di Interesse Chimico" funds ex 40%) and from the University of Bologna (Funds for Selected Research Topics) is gratefully acknowledged.

## References and Notes

(1) Laane, J. *J. Phys. Chem. A* **2000**, *104*, 7715−7733.
(2) Duckett, J. A.; Smithson, T. L.; Weiser, H. *Chem. Phys. Lett.* **1979**, *64*, 261−264.
(3) Alves, A. C. P.; Hollas, J. M.; Midmore, B. R. *J. Mol. Spectrosc.* **1979**, *77*, 124−132.
(4) Hassan, K. H.; Hollas, J. M. *Chem. Phys. Lett.* **1989**, *157*, 183−188.
(5) Caminati, W.; Melandri, S.; Corbelli, G.; Favero, L. B.; Meyer, R. *Mol. Phys.* **1993**, *80*, 1297−1315.
(6) Sakurai, S.; Meinander, N.; Morris, K.; Laane, J. *J. Am. Chem. Soc.* **1999**, *121*, 5056−5062.
(7) Sakurai, S. Ph.D. Thesis, University of Texas A and M, 1998.
(8) Laane, J.; Sakurai, S.; Klots, T.; Meinander, N.; Morris, K.; Chiang, W. Y.; Bondoc, E. *J. Mol. Struct.* **1999**, *480*−*481*, 189−196.
(9) Laane, J.; Bondoc, E.; Sakurai, S.; Morris, K.; Meinander, N.; Choo, J. *J. Am. Chem. Soc.* **2000**, *122*, 2628−2634.
(10) Pietraperzia, G.; Zoppi, A.; Becucci, M.; Droghetti, E.; Castellucci, E. *Chem. Phys. Lett.* **2004**, *385*, 304−308.
(11) Meyer, R. *J. Mol. Spectrosc.* **1979**, *76*, 266.
(12) Kisiel, Z.; Pszczolkowski, L.; Pietraperzia, G.; Becucci, M.; Caminati, W.; Meyer, R. *Phys. Chem. Chem. Phys.* **2004**, *6*, 5469−5475.
(13) Bondoc, E. Ph.D. Thesis, University of Texas A and M, 1999.
(14) Moon, S.; Kwon, Y.; Lee J.; Choo, J. *J. Phys. Chem. A* **2001**, *105*, 3221−3225. Choo, J. *J. Mol. Struct.* **2001**, *597*, 235−240.
(15) Roos, B. O. In *Ab Initio Methods in Quantum Chemistry*; Lawley, K. P., Ed.; Advances in Chemical Physics II; John Wiley & Sons Ltd.: Chichester, England, 1987; Vol. LXIX, p 399.
(16) Andersson, K.; Barysz, M.; Bernhardsson, A.; Blomberg, M. R. A.; Carissan, Y.; Cooper, D. L.; Cossi, M.; Fleig, T.; Fülscher, M. P.; Gagliardi, L.; de Graaf, C.; Hess, B. A.; Karlström, G.; Lindh, R.; Malmqvist, P.-Å.; Neogrády, P.; Olsen, J.; Roos, B. O.; Schimmelpfennig, B.; Schütz, M.; Seijo, L.; Serrano-Andrés, L.; Siegbahn, P. E. M.; Stålring, J.; Thorsteinsson, T.; Veryazov, V.; Wierzbowska, M.; Widmark, P.-O. *MOLCAS*, version 5.2; Dept. of Theor. Chem., Chem. Center, University of Lund: Lund, Sweden, 2001.
(17) Duschinsky, F. *Acta Physicochim. URSS* **1937**, *1*, 551.
(18) Herzberg, G. *Electronic Spectra and Electronic Structure of Polyatomic Molecules*; Van Nostrand: Princeton, NJ, 1967; Chapter 2.
(19) Orlandi G.; Siebrand, W. *J. Chem. Phys.* **1973**, *58*, 4513−4523.
(20) Manneback, C. *Physica* **1951**, *17*, 1001−1010. Siebrand, W. *J. Chem. Phys.* **1967**, *46*, 440−447.